

LHC-VAC/IRC

Vacuum Technical Note 98-04
March 1998

Room Temperature Measurements of the Molecular Photodesorption Yields from a TiZr Getter Film.

V. Baglin, I. R. Collins, O. Gröbner and F. Le Pimpec

Abstract

Effective photodesorption yields of a TiZr film at room temperature after various surface conditionings, namely, as-received, baked at 120°C, 250°C, 350°C and after saturation with $4 \cdot 10^{15}$ CO molecules per square centimetre were made on a dedicated beamline on the EPA ring at CERN. Measurements were performed using a synchrotron radiation spectrum with 45 and 194 eV critical energy at a mean incidence angle of the photon beam of 11 mrad. The molecular species desorbed were H₂, CH₄, H₂O, CO, O₂ and CO₂. The results suggest that the getter surface is not fully activated at 250°C and when conditioned at the temperature of 350°C a sticking coefficient for hydrogen of about $4 \cdot 10^{-2}$ can be deduced. Effective photodesorption yields as well as an estimation of the intrinsic (primary) photodesorption yields are presented. These data have been introduced into the present model of the dynamic evolution for H₂ in the cold arc of the LHC and indicate that the beam lifetime limit for a NEG pumped beam screen will be reached within 10 hours of nominal machine operation.

1. Introduction

Non-Evaporable Getter (NEG) coatings of the internal surface of vacuum chambers have been studied intensively at CERN for several years in view of their future application in accelerators [1]. NEG's are attracting increasing interest since, in principle, they provide an elegant solution for distributed pumping in conductance limited vacuum systems and vacuum systems with a high gas load such as storage rings with intense synchrotron radiation. In the LHC, and in other machines with intense beams of positively charged particles, the dynamic pressure increase and specifically the ion induced pressure bump instability pose serious problems which must be solved by providing simultaneously a clean surface and large effective pumping speeds. A very attractive application of a continuous getter pump in the LHC are the experimental beampipes where the detectors must be located as close as possible to the interaction point thereby imposing, over a considerable length of the experiment, a beam pipe with a minimum diameter and hence with a low vacuum conductance. Nevertheless, getter pumping requires that the activation of the film can be made *in-situ* whenever the pumping capacity has been saturated and it has been proposed that this step becomes part of a conventional bakeout in case the temperature required for activation can be lowered to an acceptable value.

One of the promising types of NEG's under study has been the equiatomic TiZr alloy since it was found to have an activation temperature (200-250°C) which is low compared to the commercially available pumping strips coated with St101 (700°C [2, 3] as used in LEP) and the St707 (~300°C [4]). Such a getter could therefore be used for experimental vacuum chambers fabricated from a special Al alloy (*e.g.* type 2219 [5]) bakeable up to 250°C.

With particular reference to the LHC, it has furthermore been suggested to coat not only the experimental beampipes and the adjacent bakeable room temperature sections of the vacuum system with such a getter film but to extend this pumping principle also into the cold arcs. In this case a bakeable NEG coated beam screen would become a vacuum tight separation between the beam vacuum and the insulation vacuum in the bore of the magnet cold masses. As a consequence the cryopumping,

with virtually an infinite capacity, of the beam vacuum by the 1.9 K cold bore would no longer be possible.

In the design of the vacuum system for the LHC, it is important to quantify photon stimulated desorption since, in particular, the arcs of the machine will be subject to intensive photon irradiation (about 10 times higher photon flux than in LEP). The effect of the synchrotron radiation in LHC with a critical energy of 45 eV has been studied extensively over the last few years and a complete set of data exists for conventional vacuum chamber materials like Cu and stainless steel [6, 7, 8]. The purpose of this study has been to obtain first results for the photon induced molecular desorption from a TiZr film deposited on a 316 L stainless steel chamber using the existing photon beam line on the EPA ring at 45 eV and at 194 eV critical energies.

2. Experimental details

2.1. Experimental system

A schematic of the beamline, used previously for studying Al, Cu and stainless steel materials [9], is shown in Figure 1. The synchrotron radiation enters the beamline through a square collimator (11 x 11 mm) which defines a beam divergence of ± 3.9 mrad. During the experiment the test chamber is irradiated at a mean incidence angle of 11 mrad with either 45 eV or 194 eV critical energy synchrotron radiation. Due to the vertical collimation, photon energies below ~ 4 eV only are attenuated.

The test chamber is pumped through a conductance of 72.5 l s^{-1} for nitrogen by a combination of a 270 l s^{-1} for nitrogen sputter ion pump and two titanium sublimation pumps. The total pressure is measured with a calibrated Bayart-Alpert gauge (BA1) and the partial pressures by a calibrated Residual Gas Analyser (RGA).

A gate valve, labelled 'isolation valve' in Figure 1, provides the possibility of inter-changing test chambers without venting the front part of the system. Furthermore, a test chamber can be isolated from the pumping system and exposed to controlled quantities of gas which is injected from a calibrated volume ($V=1.075$ litres) at a known pressure.

A machined OFHC Cu collector and a stainless steel wire electrode were mounted in the test chamber to measure the photon reflection and the photoelectron yield of the test chamber surface, respectively [10].

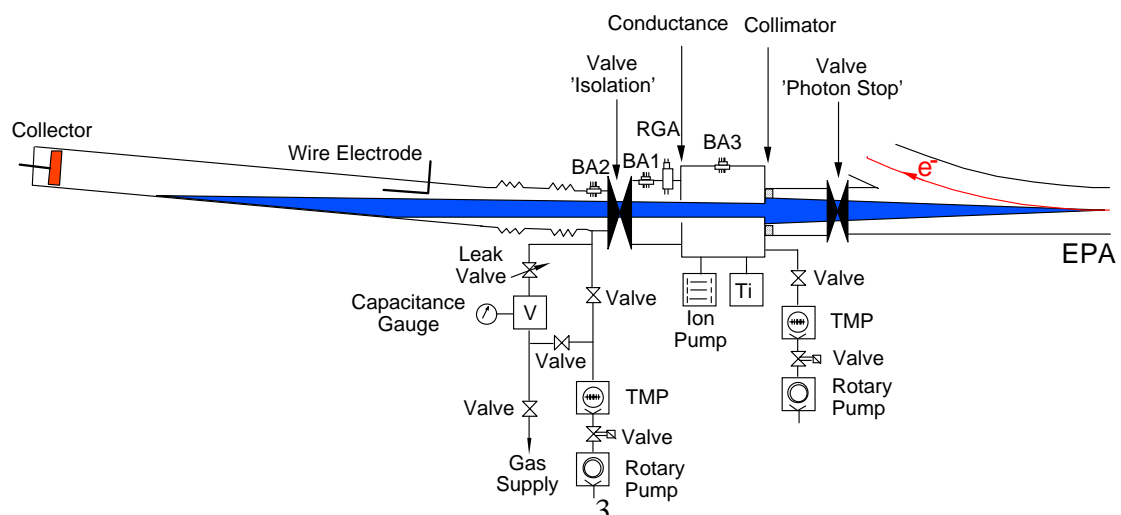


Figure 1: Schematic of EPA beamline

2.2. Test chamber preparation

The 4 m long, 100 mm diameter stainless steel (316 L) test chamber (two sections each two metres long) was coated with $\sim 1 \mu\text{m}$ TiZr getter film by the EST-SM Group. Some basic vacuum properties of similar films have been reported previously in Ref. 1. *In-situ* bakeout was achieved with conventional bakeout jackets. During bakeout the isolation valve was closed and the test chamber pumped by a 60 l s^{-1} turbomolecular pump. Consequently only the front part of the vacuum system and the test chamber needed to be heated.

The test chamber was studied with 5 different surface conditionings, chronologically: as-received, baked at 120°C , 250°C and 350°C and finally exposed to 2 Torr l of CO. Details of these steps are given below:

1) The as-received test chamber was evacuated for 13 hours to obtain a sufficiently low base pressure, $5 \cdot 10^{-8}$ Torr (mainly H_2O), before starting the photodesorption measurements.

2) The test chamber was baked at 120°C for 12 hours, a temperature high enough to remove water but low enough not to activate the NEG film, resulting in a base pressure of $7 \cdot 10^{-10}$ Torr, 3.5 h after bakeout. H_2 was the dominant residual gas.

3) The test chamber was baked at 250°C for 9 hours; the isolation valve and the turbomolecular pump were maintained at 200°C . The base pressure, 5 hours after bakeout and before irradiation, was $4 \cdot 10^{-10}$ Torr. H_2 was again the dominant residual gas.

4) In the final step, the test chamber was baked at 350°C for 6 hours. Unfortunately, after bakeout, the RGA indicated that a leak had appeared and during the leak search the chamber was accidentally vented to 10^{-5} Torr. In spite of an extensive search, no leak could be found. Within the limited machine time available, the chamber was re-baked, initially at 125°C for 11 hours to remove the water, followed by conditioning at 160°C for 6 hours and, finally, followed by 350°C for 10 hours. During these thermal conditionings, the isolation valve, the turbomolecular pump and the front end were only baked to 120°C . The base pressure, 36 h after bakeout was $5 \cdot 10^{-11}$ Torr. The spectrum was dominated by H_2 .

5) To complete the programme, 2 Torr l of CO were injected into the test chamber and remained there for 17 hours during which time the pressure in the chamber was in the range of $2 \cdot 10^{-3}$ to 10^{-2} Torr. On opening of the isolation valve, the pressure at BA1 was 10^{-6} Torr after 1 hour of pumping and decreased to $2 \cdot 10^{-10}$ Torr after firing the Ti sublimators and two additional hours of pumping. In this situation, the spectrum was dominated entirely by CO. From the pressure readings before the evacuation one can deduce that the surface was covered with approximately 4 monolayers, corresponding to $4 \cdot 10^{15}$ CO molecules cm^{-2} .

All photodesorption measurements were made at room temperature. In order to minimise a cumulative cleaning effect and to obtain the initial photodesorption yields, the accumulated dose during each irradiation was kept as low as possible (of the order of $2 \cdot 10^{19}$ photons m^{-1}).

Unfortunately, post measurement inspection when the system was finally dismantled indicated that during step 4, the actual temperatures must have exceeded by far the desired values over a short length of the chamber (~550 °C as judged by the local colour of the steel, possibly due to a defective bakeout equipment). Local overheating has also been detected at the location of the Cu collector.

3. Photodesorption results

The photodesorption yield η (molecules photon⁻¹) of a conventional vacuum chamber at room temperature is given by the conductance method, *i.e.*:

$$\eta = \frac{G C \Delta P}{\dot{\Gamma}} \quad (1)$$

where ΔP (Torr) is the increase of pressure under photon bombardment, C is the pumping speed of the conductance (l s⁻¹), $\dot{\Gamma}$ is the photon flux (photons s⁻¹) and G is a constant converting Torr l into molecules.

The relation (1) gives the exact photodesorption yield under the condition that the pressure in the pumping station is small compared to the pressure in the test chamber, note that $P_{BA1} \sim 10 P_{BA3}$ in our experimental set-up. This method is valid for the unbaked TiZr case. However, when the TiZr getter film is activated the test chamber acts itself as a pump and this condition may no longer be met. Under these circumstances it is necessary to use both gauges BA1 and BA3 to calculate the flow of gas through the conductance. Unfortunately the flux passing the conductance for each gas cannot be evaluated since there is no RGA in the pumping chamber of our system. Total pressure measurements indicate that an overestimation in the total effective photodesorption yields of 20%, 50% and 30 %, for 250°C bakeout, 350°C bakeout and CO exposure, respectively, can be made due to this effect. Furthermore, when the wall of the test chamber pumps, the measured effective photodesorption yield is the result of a competition between photodesorption and pumping by the getter and among others, depends on the geometry and the conductances of the system. Indeed, it is easy to understand that if molecules are desorbed far from the conductance near the collector, they have less chance to reach the gauge, BA1, than molecules desorbed near entrance of the test chamber.

In this context it is worth noting that even with an activated test chamber in the straight-through position, when the photons strike only the end collector, the pressure rise measured on the gauge BA1, four metres upstream, was still significant. This observation suggests that the sticking coefficient of the desorbed molecules must be relatively low.

3.1. Reflected photons

Due to their grazing incidence on the side of the test chamber, some photons are reflected and irradiate the Cu collector at the end giving rise to some additional, parasitic desorption. In order to determine this contribution, the collector was irradiated at normal incidence for each conditioning state and the corresponding effective photodesorption yield η_{Col} was determined. Using the measured photon reflectivity, R , of the TiZr coating corresponding to 0.2 and 0.17 for the 45 eV and 194

eV critical energy spectrum respectively, and assuming that these values remain constant throughout the series of measurements [10], this contribution to the global desorption has been subtracted from the raw data to obtain the effective photodesorption yield, η_{TiZr}

$$\eta_{\text{TiZr}} = \eta - R \eta_{\text{Col}} \quad (2)$$

The correction due to the end collector is at most 30%.

3.2. Wall pumping and sticking probability

The wall pumping speed of the test chamber has been calculated in this experiment using the fact that the photodesorption of the end collector is known. Assuming, in addition that it represents a constant flow of gas into the test chamber and comparing the pressure rise ΔP_1 for a test chamber which has not been activated with the corresponding pressure rise ΔP_2 of the activated chamber, the average wall pumping speed, S , and hence the sticking probability, σ , on the getter coating can be calculated from the expression

$$S = C \left(\frac{\Delta P_1}{\Delta P_2} - 1 \right) \quad (3)$$

Here C is the conductance of the pumping orifice.

The deduced sticking coefficients for the geometrical getter surface area of 12566 cm^2 are shown in Table 1. It should be noted that the calculated sticking coefficients assume a constant ΔP_1 , independent of surface conditioning. Any surface cleaning due to subsequent baking at higher temperatures, which would reduce ΔP_1 , would tend to give lower values for the sticking coefficients. Nevertheless, comparison of these data with results for H_2 and CO at 250°C and 300°C which can be inferred from Ref. 1 shows good agreement to within 40% for 250°C and $\sim 70\%$ for 350°C . After exposure to CO the sticking coefficients of all detected gases decrease, in particular significant reductions are found for H_2 and CO , as can be seen in the last column in Table 1. In spite of this saturation CO exposure, the sticking probability for CO remains significantly larger than zero.

As a final remark, since the sticking probability for CH_4 can be expected to be zero, an estimate of the experimental error of the order of 0.005 can be inferred from the data in Table 1.

Table 1: Sticking coefficients for a TiZr coating at room temperature.

Gas	Surface conditioning				
	Unbaked	Baked at 120°C	Baked at 250°C	Baked at 350°C	Baked at 350°C + CO saturation
H_2	0.000	0.000	0.002	0.044	0.002
CH_4	0.000	0.000	0.002	0.005	0.004

H ₂ O	-	-	0.010	0.009	0.005
CO	0.000	0.000	0.062	0.190	0.022
O ₂	-	0.000	-	0.003	-
CO ₂	0.000	0.000	0.363	0.436	0.280

3.3. Effective photodesorption yields at 45 eV critical energy

Figure 2 shows the effective photodesorption yield of the test chamber for a critical energy of 45 eV as a function of the five different surface conditionings.

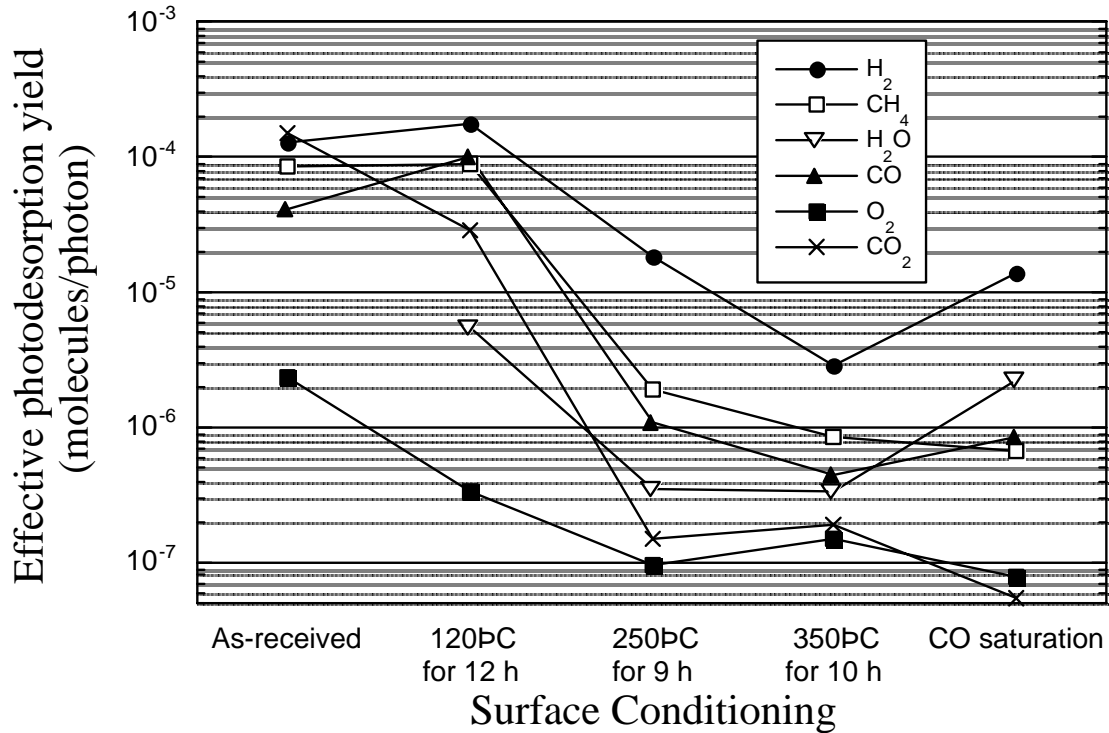


Figure 2: Effective photodesorption yield of the test chamber at 45 eV critical energy.

The photodesorption yields for the unbaked chamber are comparable to within 10 to 50% with previous measurements made on unbaked stainless steel [11]. In the unbaked condition, the pressure increase of H₂O above the background level was, however, too small to be resolved and thus this yield is not shown.

To measure the desorption yield for H₂O baking to 120°C was required in order to reduce the background pressure sufficiently. In comparison with the unbaked case H₂ and CH₄ remain essentially unchanged. On the other hand, the CO yield increases by a factor of 2.5 while the values for O₂ and CO₂ are reduced by factor of 7 and 6 respectively. This observation could indicate that the getter film is partially active for these gases.

For bakeout temperatures of 250°C and higher, a strong reduction of the effective photodesorption yields are observed as may be expected due to the increased pumping speed of the getter film.

Activation at 350°C reduces the effective photodesorption yield of H₂ by one order of magnitude compared to that at 250°C indicating that the NEG coating was not fully activated at 250°C.

A saturation CO exposure of the TiZr film results not only in an increase of the effective photodesorption yield for CO but also increases the effective yields of H₂ and H₂O. This observation agrees with pumping speed measurements in the laboratory

[12]. However, it should be noted that the gas injection line was not baked and therefore the injection of these contaminant gases cannot be excluded.

3.4. Effective photodesorption yields at 194 eV critical energy

Figure 3 shows the effective photodesorption yields for the different surface conditionings of the test chamber at 194 eV critical energy.

For the unbaked case, the results are again in agreement to within 10 to 50%, with previous measurements [11]. The increase of the H₂O signal was again too small to be measured, and thus its yield is not plotted for the unbaked case.

The same trends as in the 45 eV critical energy data can be seen although the effective photodesorption yields are in general a factor 2 to 5 higher.

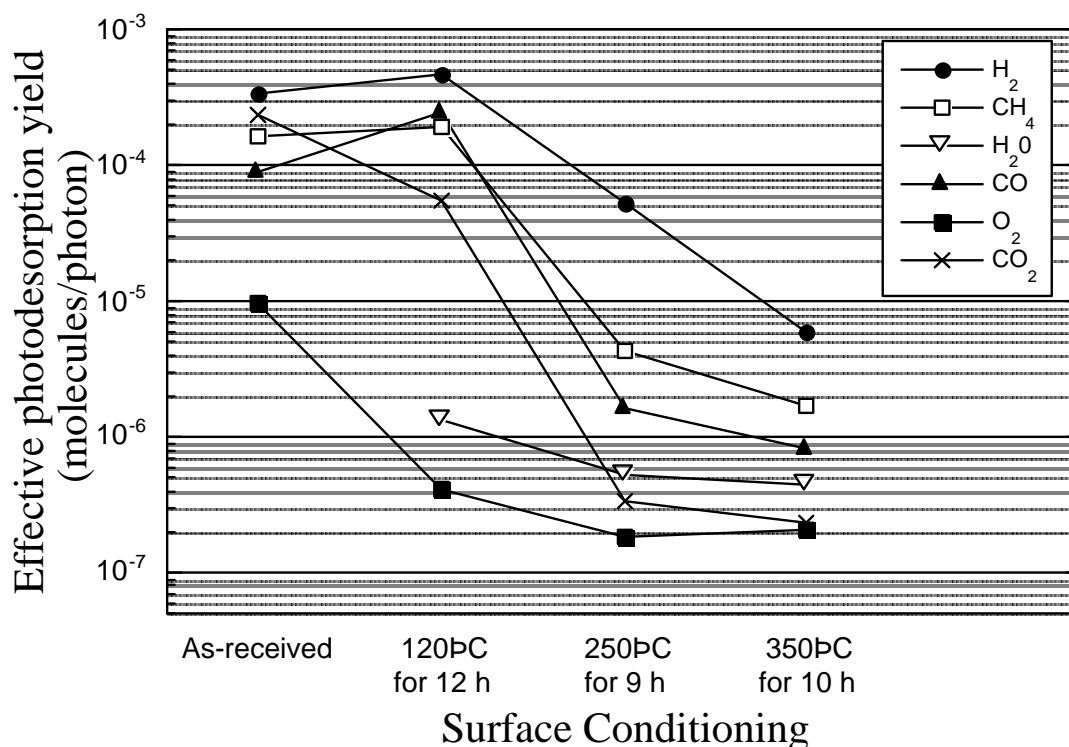


Figure 3: Effective photodesorption yields at 194 eV critical energy.

4. Estimation of the intrinsic photodesorption yield

In the same way as it has been discussed in previous work on cryosorbing surfaces [6], the effective desorption yield measured in this work represents the combined effect of the primary desorption yield and of the sticking probability of molecules on the wall.

When the test chamber is activated, *i.e.* at bakeout temperatures exceeding 120°C, photodesorbed molecules which can be detected at the conductance C are the result of the competition between photodesorption and pumping of the TiZr getter film. Since the sticking probability on the getter film for the different gas species can be derived by an independent measurement this sticking coefficient has subsequently been

used to separate the two effects and thus to calculate the intrinsic photodesorption yield.

Indeed, using a model for a uniform wall pumping [13] along the test chamber, depicted in Figure 4, one can calculate a correction factor, f ,

$$f = \frac{S}{C} + \sqrt{\frac{S}{C_t}} \quad (4)$$

which converts the measured effective photodesorption yield to the intrinsic, primary photodesorption yield (see appendix).

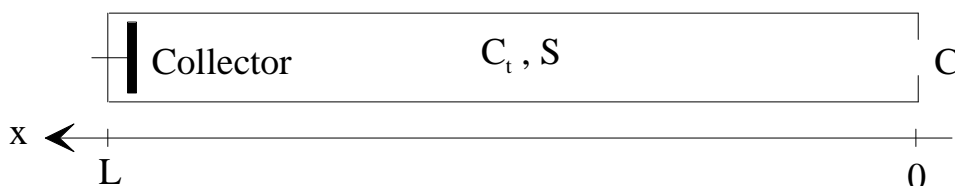


Figure 4: Geometry used in the model. The test chamber of length, L , has a conductance, C_t , and a wall pumping speed, S . Molecules desorbed from the collector are measured as they pass through the pumping orifice with the conductance C . Thermal outgassing of the test chamber is neglected.

Table 2 summarises, for the critical energy of 45 eV, the effective photodesorption yield, η_{TiZr} , the correction factor, f and the primary, intrinsic photodesorption yield, $\eta_{\text{intrinsic}}$ for the different surface conditionings.

Figure 5 shows the intrinsic photodesorption yield for synchrotron radiation of 45 eV critical energy. For all measurements, with the exception of CH_4 , the intrinsic photodesorption yields remain nearly constant, *i.e.* no strong dependence on the surface conditioning. For CH_4 the intrinsic photodesorption yield is found to decrease during the series of measurements but this effect may most likely be attributed to the cumulative effect of the successive bakeouts. Comparison of these intrinsic photodesorption yields with corresponding data for unbaked stainless steel [11] shows in fact no significant differences to within 50 %. It is interesting to note that, after the CO saturation of the getter surface, the intrinsic photodesorption yields for all gases except H_2O appears to be reduced.

Table 2: Compilation of the effective photodesorption yield, correction factor and primary, intrinsic photodesorption yield for the 45 eV critical energy for the different surface conditionings of the test chamber.

Surface conditioning	H ₂	CH ₄	H ₂ O	CO	O ₂	CO ₂
	η_{TiZr} f	η_{TiZr} f	η_{TiZr} f	η_{TiZr} f	η_{TiZr} f	η_{TiZr} f
	$\eta_{\text{intrinsic}}$	$\eta_{\text{intrinsic}}$	$\eta_{\text{intrinsic}}$	$\eta_{\text{intrinsic}}$	$\eta_{\text{intrinsic}}$	$\eta_{\text{intrinsic}}$
Baked at 250°C	1.8 10 ⁻⁵	1.9 10 ⁻⁶	3.5 10 ⁻⁷	1.1 10 ⁻⁶	9.5 10 ⁻⁸	1.5 10 ⁻⁷
	6	8	27	141	-	771
	1.1 10 ⁻⁴	1.5 10 ⁻⁵	9.4 10 ⁻⁶	1.5 10 ⁻⁴	-	1.1 10 ⁻⁴
Baked at 350°C	2.9 10 ⁻⁶	8.5 10 ⁻⁷	3.3 10 ⁻⁷	4.4 10 ⁻⁷	1.5 10 ⁻⁷	1.9 10 ⁻⁷
	104	15	24	327	10	922
	3.1 10 ⁻⁴	1.3 10 ⁻⁵	7.7 10 ⁻⁶	1.4 10 ⁻⁴	1.5 10 ⁻⁶	1.7 10 ⁻⁴
Baked at 350°C + CO saturation	1.4 10 ⁻⁵	6.7 10 ⁻⁷	2.2 10 ⁻⁶	8.6 10 ⁻⁷	-	5.5 10 ⁻⁸
	6	12	16	54	-	599
	9.1 10 ⁻⁵	7.7 10 ⁻⁶	3.6 10 ⁻⁵	4.6 10 ⁻⁵	-	3.3 10 ⁻⁵

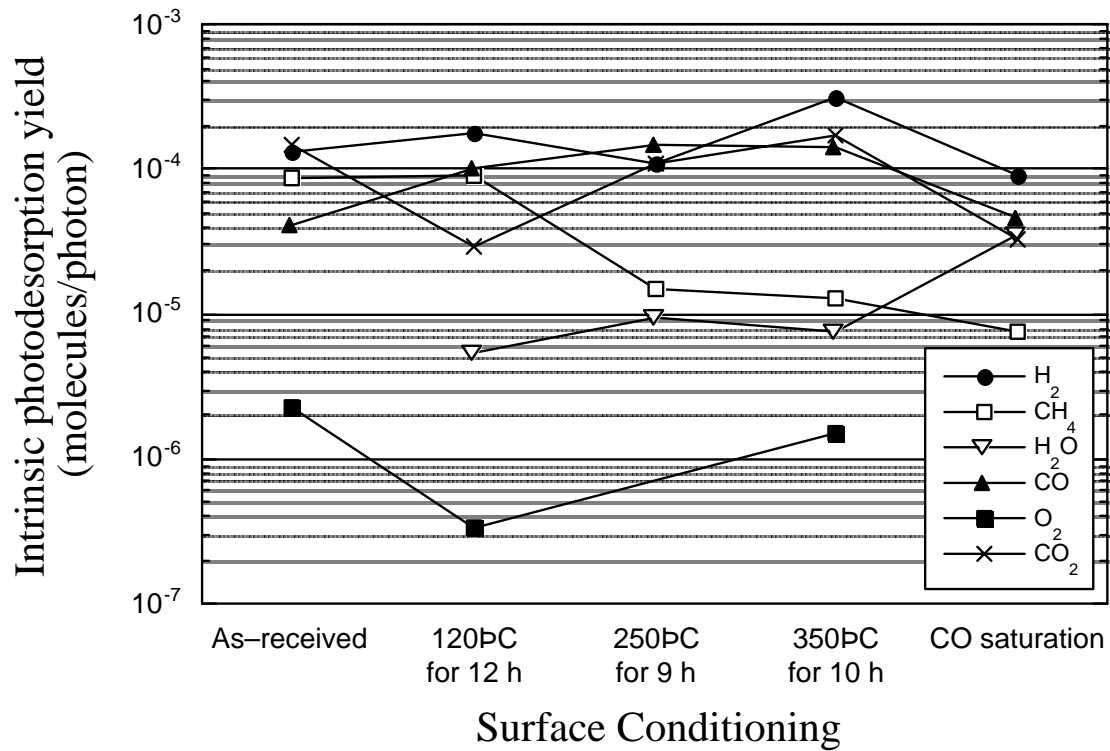


Figure 5: Intrinsic photodesorption yield after different conditionings of the test chamber for 45 eV critical energy synchrotron radiation.

5. Dynamic vacuum in a cold arc of the LHC

The preliminary data shown in Table 2 have been used with the present model of the dynamic pressure evolution for H_2 in the cold arc of the LHC. The details of this model and its comparison with measurements on a Cu-coated beam screen with pumping holes have been described previously [6]. Here, it has been assumed that the beam screen has no pumping holes and that at the temperature below 20 K the getter coated beam screen would pump only by physisorption on its surface. Diffusion into the bulk is assumed to be negligible at this temperature. Furthermore, in the absence of direct measurements, the recycling coefficient for the physisorbed H_2 molecules has been assumed to be the same as for a Cu substrate.

Figure 6 shows the hydrogen density in a beam tube at 4.2 K as a function of the photon dose, *i.e.* running time with nominal beam conditions. There it can be seen that due to the increasing coverage of the physisorbed H_2 and the proportional increase of the recycled gas, the beam lifetime limit in the LHC (corresponding to $10^{15} H_2 m^{-3}$) is reached within ten hours *i.e.* before the vapour pressure becomes the dominant contribution.

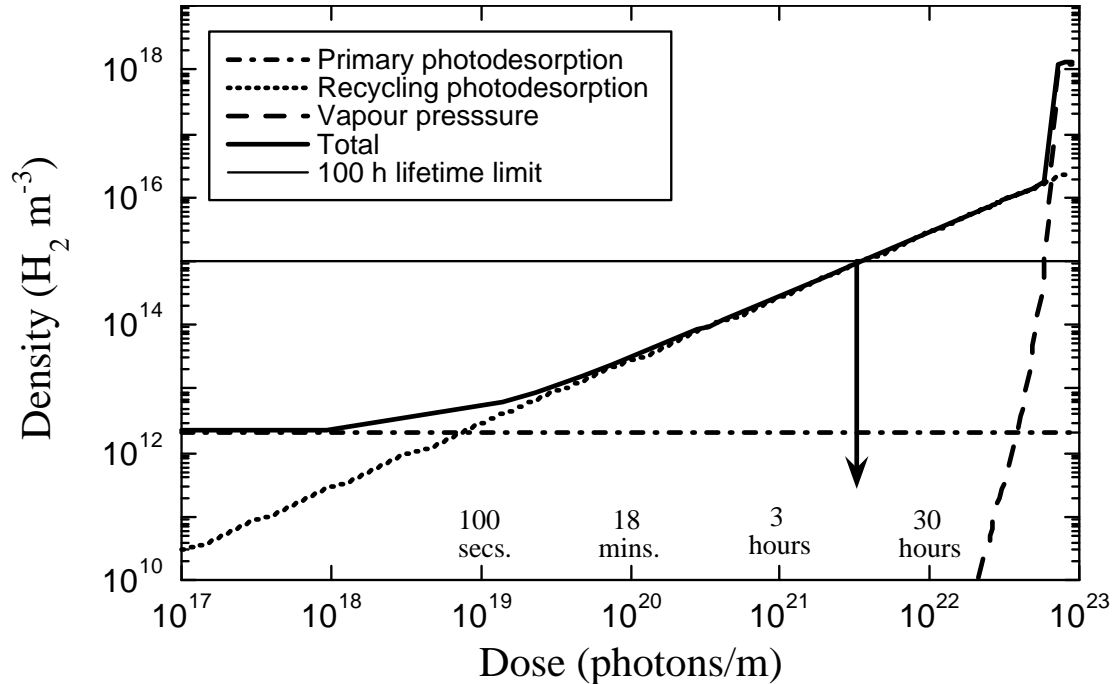


Figure 6 : Hydrogen density in an infinitely long TiZr coated beam tube at 4.2 K. The horizontal dashed-dotted line gives the pressure rise due to the constant primary desorption ($\eta = 10^{-4}$ molecule.photon $^{-1}$ *i.e.* no beam cleaning taken into account). The dotted curve represents the contribution of the recycling of physisorbed gas ($\eta' = 1$ molecule.photon $^{-1}$.monolayer $^{-1}$). The sticking coefficient is assumed to be constant and equal to 0.6, as in previous work [6], and the monolayer coverage is assumed to be $5 \cdot 10^{19}$ molecules.cm $^{-2}$.

6. Summary

First results of photon induced molecular desorption from a test chamber coated with a TiZr getter film have been obtained. However, due to several incidents

during the experiment, these data should be considered as very preliminary. The chamber has been irradiated with synchrotron radiation of 45 and 194 eV critical energy following surface conditionings at temperatures up to 350°C. Results show that H₂, CH₄, H₂O, CO, O₂ and CO₂ were photodesorbed in significant quantities independent of the conditioning temperature. The photodesorption yields measured in the unbaked case were typically those measured previously with unbaked stainless steel. Bakeout at temperatures of 250°C and above decreases the effective photodesorption yield by ~ two orders of magnitude in line with the expected increase of the wall pumping speed due to the activation of the TiZr getter. Measurements of the sticking probabilities on the TiZr film have been made and give values of about $4 \cdot 10^{-2}$ for H₂ and about $2 \cdot 10^{-1}$ for CO when the getter is activated at 350°C. After saturation of the getter film with $4 \cdot 10^{15}$ CO cm⁻² an increase of the effective desorption yield for H₂ by approximately one order of magnitude has been observed. The intrinsic photodesorption yield for the different molecular species derived from these measurements, taking account of the respective sticking probabilities on the wall of the test chamber, range between 10^{-5} and 10^{-4} molecules photon⁻¹. The measured primary desorption yield for H₂ has been used with the present dynamic pressure model of the LHC for a getter coated beam screen without pumping holes. This model which assumes physisorption of H₂ only shows that the beam lifetime limit of 10^{15} molecules m⁻³ would be reached within about 10 hours at the nominal beam conditions.

Acknowledgements

The assistance of D. Jenson is gratefully acknowledged. We would like to thank C. Benvenuti, P. Chiggiato and V. Ruzinov for coating the test chamber with the TiZr getter film. We are grateful to L. Rinolfi and his operating crew for running the EPA machine at the reduced beam energy to provide the LHC conditions.

Appendix

To compute the correction factor, f , a model based on a uniform wall pumping speed has been used [14].

When the test chamber is uniformly irradiated along its length, the pressure profile $P(x)$ along the chamber with length, L , and with a wall pumping speed, S , (see Figure 4) is defined by the differential equation :

$$L C_t \frac{d^2 P}{dx^2} = \frac{S}{L} P(x) - \lambda \quad (5)$$

where :

L is the length of the chamber (m)

C_t is the conductance ($l\ s^{-1}$)

S is the wall pumping speed ($l\ s^{-1}$)

λ is the uniformly distributed gas load due to photodesorption per unit length ($\text{Torr}\ l\ s^{-1}\ m^{-1}$)

The general solution of this equation is :

$$P(x) = P_0 + k_1 e^{\omega x} + k_2 e^{-\omega x} \quad (6)$$

where:

$$P_0 = \frac{\lambda L}{S} \text{ (Torr)}$$

k_1 and k_2 are dimensionless constants defined by the appropriate boundary condition and

$$\omega = \sqrt{\frac{S}{L^2 C_t}} \text{ (m}^{-1}\text{)} .$$

In our set-up the pressure, P_{ch} , is measured at the location of the conductance C (assumed to be a perfect pump) and the pressure distribution has its maximum at $x = L$. This defines two boundary conditions :

$$\begin{cases} L C_t \frac{dP(x)}{dx} \Big|_{x=0} = P_{ch} C \\ \frac{dP(x)}{dx} \Big|_{x=L} = 0 \end{cases}$$

thus the pressure measured at the conductance can be expressed as :

$$P_{ch} = P_0 \tanh(\omega L) \frac{\sqrt{C_t S}}{C + \sqrt{C_t S} \tanh(\omega L)} \quad (7)$$

For sufficiently large values of ωL (*i.e.* corresponding to a sticking coefficient $\sigma \geq 0.0007$) the expression can be simplified:

$$P_{\text{Ch}} = \frac{\lambda L}{S + C \sqrt{\frac{S}{C_t}}} \quad (8)$$

The flux q measured at the conductance is :

$$q = C P_{\text{Ch}} = C \frac{\lambda L}{S + C \sqrt{\frac{S}{C_t}}} \quad (9)$$

To obtain the intrinsic photodesorption yield, λL , the effective photodesorption yield, q , has to be multiplied by the factor, f :

$$f = \frac{S}{C} + \sqrt{\frac{S}{C_t}} \quad (10)$$

References

- [1] C. Benvenuti, P. Chiggiato, F. Cicoira, Y. L'Aminot. Internal Note EST-SM 97-01 (1997)
- [2] C. Benvenuti and F. Francia. *J. Vac. Sci. Technol.* **A 6**, 2528 (1988).
- [3] C. Benvenuti and F. Francia. *J. Vac. Sci. Technol.* **A 8**, 3864 (1990).
- [4] C. Benvenuti and P. Chiggiato. *J. Vac. Sci. Technol.* **A 14**(6), 3278 (1996).
- [5] S. Sgobba, private communication.
- [6] R. Calder, O. Gröbner, A. G. Mathewson, V. V. Anashin, A. Dranichnikov, O. B. Malyshev. *J. Vac. Sci. Technol.* **A 14**(4), 2618 (1996).
- [7] V. V. Anashin, O. B. Malyshev, V. N. Osipov, I. L. Maslennikov, W. C. Turner. *J. Vac. Sci. Technol.* **A 12**(5), 2618 (1994).
- [8] V. Baglin, Ph.D. Thesis, University D. Diderot Paris 7 (1997).
- [9] J. Gómez-Goñi, O. Gröbner, and A. G. Mathewson. *J. Vac. Sci. Technol.* **A 12**(4), 1714 (1994).
- [10] I. R. Collins, V. Baglin and O. Gröbner, to be published.
- [11] J. Gómez-Goñi, O. Gröbner, A. G. Mathewson and A. Poncet, CERN Vacuum Technical Note 92-02, (1992).
- [12] P. Chiggiato, private communication.
- [13] C. Herbeaux, P. Marin, V. Baglin and O. Gröbner, LURE RT/97-03.
- [14] J. M. Laurent, Vacuum Technical Note 94-20 (1994).